Ultrahigh Strength of Dislocation-Free Ni_3Al Nanocubes

Robert Maaß, Lucas Meza, Bin Gan, Sammy Tin, and Julia.R. Greer*

Defect-free crystals of all sizes generally require the application of close-to-theoretical stresses for the initiation of plastic deformation. Testing this classical tenet is challenging in bulk or even in microsized samples because defects naturally emerge during either crystal growth or sample fabrication. At the nanoscale, however, it is possible to create dislocation-free mechanical specimens, enabling either confirmation or refutal of this classical hypothesis. Here, we investigate the compressive strengths of both dislocation-free and Ga^+-irradiated Ni_3Al nanocubes. Combined with data for other dislocation-free face-centered cubic nanocrystals, our results suggest a size-dependent strength in these dislocation-free samples. We discuss these findings in the framework of dislocation nucleation at free surfaces as a governing plasticity mechanism in nanosized crystals. This study sheds more light on the understanding of fundamental deformation mechanisms and the size-affected strength of pristine metallic nanocrystals.

Original work on nickel[1] micropillars and gold[2] nanopillars has clearly established that single-crystalline metallic micro- and nanostructures considerably outperform their macroscopic counterparts in strength; a principle that is found to be valid for both face-centred (fcc) and body-centred (bcc) cubic metals. While both families of metals display power-law-like strengthening, they are distinct from one another.[3,4] Proposed explanations for the differences in their size-dependent strengths revolve around the concept of fundamentally different dislocation mechanisms in each crystal type: for example, the relative mobility of screw- versus edge-components of dislocations in bcc crystals leading to multiplication and dislocation debris formation,[5] and dislocation starvation followed by surface nucleation in fcc structures.[6] Numerous reports have aided in gaining a fundamental understanding of the physical mechanisms responsible for the size-induced strengthening in single-crystalline micro- and nanomaterials.[7–14] In particular, specialized in-situ transmission electron microscopy (TEM)[15–17] and in-situ synchrotron techniques[18–21] have allowed real-time insights into the microstructural deformation characteristics at the nano- and micrometer-scale, respectively. One commonality in these studies is the use of focused ion beam (FIB) techniques to prepare both compressive and tensile specimens. While versatile and effective, this nearly ubiquitous mechanical sample preparation technique inevitably introduces defects into the sample surface. The influence of FIB milling on the mechanical response was a heavily debated topic[22–25] until it was demonstrated that the size effect in strength is prevalent for all types of dislocation/defect-containing fcc crystals regardless of the fabrication route.[26,27]

In contrast to dislocation-containing crystals discussed above, nanomechanical studies on dislocation-free fcc (as opposed to bcc) nanocrystals have so far only been conducted on faceted Cu whiskers,[11] revealing ultrahigh tensile strengths without any systematic trends on the order of $G/50$ to $G/11$ for Cu, where G is the shear modulus. Tensile experiments on dislocation-free Cu nanowhiskers reveal brittle fracture with no discernable plasticity. While the obtained strength data falls well within the master plot summarizing size-affected flow for dislocation-containing crystals (see, for example, reference [11], Figure 3), the length scale range is too small for conclusive understanding of whether the size effect is present in these atomically smooth crystals, urging continued research.

In addition to dislocation-free fcc nanocrystals, compression studies on dislocation-free Mo alloy bcc crystals prepared by a wet-chemical route unambiguously revealed size-independent strengths.[28] Similar to the Cu nanowhiskers, they deformed at stresses close to the theoretical stress for initiation of plastic flow, achieving critical resolved shear stresses of ca. $G/26$. Subsequent work on these bcc nanocrystals highlighted the role of the pre-existing dislocation/defect network on the nanomechanical response, i.e., a pronounced difference in the intermittent nature of plastic flow depending on the history (as-prepared, pre-strained, and intentionally ion-beam irradiated) of the specimen.[29,30] These authors show that the yield and flow response of as-prepared Mo nanocrystals is deterministic, which also appears to be the case at higher degrees (11%) of pre-straining, for which bulk-like flow is observed. Intermediate degrees of ca. 4–8% pre-straining, on the other hand, resulted, similarly to FIB prepared specimen, in a very stochastic yielding behavior and a flow response that suggests a size-dependence.[29]

Dr. R. Maaß, L. Meza, Prof. J. R. Greer
California Institute of Technology
Division of Engineering and Applied Sciences
1200 E California Blvd, Pasadena, CA 91125, USA
E-mail: maass@caltech.edu
B. Gan, Prof. S. Tin
Illinois Institute of Technology
10 W. 32nd St., Chicago, IL 60616, USA
Prof. J. R. Greer
Kavli Nanoscience Institute
California Institute of Technology
Pasadena, CA 91125, USA

DOI: 10.1002/smll.201102603

Thus at present, current research suggests *size-independent* strength for dislocation-free sub-250-nm fcc and 300-nm to 1.5-μm bcc crystals, and *size-dependent* strength for both crystal families with dimensions ranging from ~100 nm up to several micrometers, with pre-existing defects. Yet, a direct comparison investigating mechanical properties of dislocation-free versus dislocation-containing fcc nanocrystals is lacking. This is mainly based on complications in pursuing a sample preparation technique that permits the ability to directly compare dislocation-free and dislocated fcc nanocrystals as a function of size of the same material.

Here we investigate compressive strengths of dislocation-free Ni_3Al "nanocubes" obtained from a wet-chemical route, as well as of the same crystals intentionally exposed to FIB. Interestingly, the strongest samples in the dislocation-free group display stresses more than 5 GPa higher than those in the ion beam-imaged group. This highlights the previously observed "softening" effect of Ga^+-ion irradiation on the small scale mechanical properties of fcc metals.[31] We also observe extremely high normalized deformation strengths, reaching values 2 orders of magnitude higher than their bulk counterparts, equivalent to ~G/17. Further, our results on compression of nanocubes with equivalent diameters, defined as the diameter of a circle with the cubes cross-sectional area, varying between 275 and 600 nm may suggest the presence of a size effect. This finding is particularly intriguing as these Ni_3Al cubes are initially dislocation free, implying that they are expected to deform at size-independent and close-to-theoretical strengths.[28]

Free-standing Ni_3Al nanocubes (**Figure 1**a) that could be tested in compression along ⟨100⟩-direction, which is the out-of-plane normal of the cube faces[32] (Figure 1b) were isolated on a Si wafer. Prior to nanomechanical characterization both the bulk material and the extracted Ni_3Al nanocubes were investigated via TEM in order to search for pre-existing dislocations, as they were expected to be dislocation-free. Figure 1c displays a typical TEM image from an isolated Ni_3Al nanocrystal that was placed directly onto the TEM Cu grid (inset in Figure 1c). In addition, a TEM foil from the bulk material was prepared. While several bending contours are present (Figure 1d,e), no dislocation lines were identifiable and could not be observed in both bright field (BF) (Figure 1d) and dark field (DF) (Figure 1e, taken along the [013]-zone axis using the [002] diffraction spot, as indicated by the inset). The inset in Figure 1d also highlights two γ' nanocubes at a higher magnification in BF. The absence of dislocations in the γ' precipitates is in agreement with literature on Ni-based superalloys.[33,34]

Subsequently, the isolated Ni_3Al nanocubes were compressed with a Hysitron Triboscope nano-indenter, as well as with SEMentor (see Experimental Section for details) inside a scanning electron microscope (SEM). The obtained stress-displacement data of the as-extracted and dislocation-free nanocubes is shown in **Figure 2**a, where curves displaying a controlled unload and marked with an arrow are those obtained in situ. It is clear from Figure 2a that the samples first deformed elastically, followed by a catastrophic instability, with significant scatter in the yield stress: its mean value is 4.67 GPa and standard deviation (StD) is 2.73 GPa (data

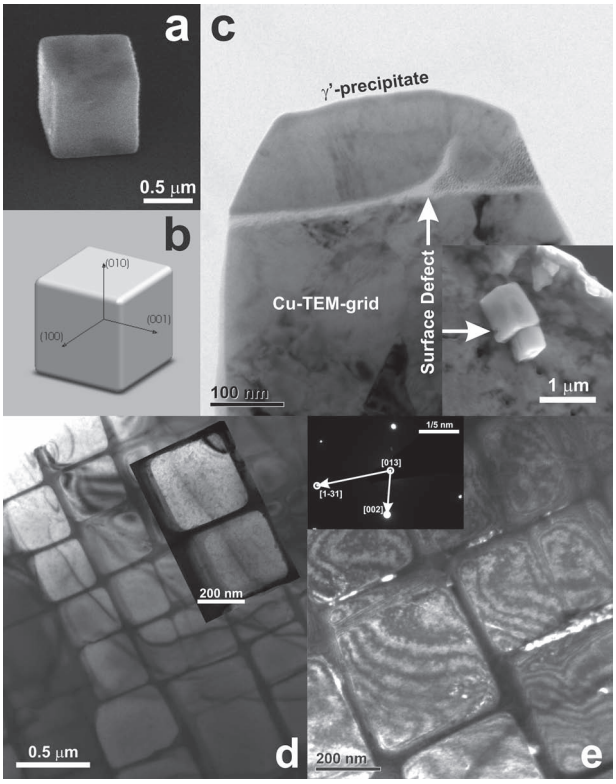

Figure 1. a) SEM image of an as-extracted Ni_3Al nanocube, with [001] out-of-plane crystallographic orientation (b). c) A bright-field TEM image is shown for an isolated as-extracted nanocrystal. The inset depicts the nanocrystal prior to FIB-thinning, and the arrow indicates a pre-existing shape imperfection. d) Bright-field TEM image of the as-received bulk material. The inset in (d) shows zoomed-in images of two adjacent γ' nanocubes from the as-received material. e) Dark-field TEM image taken along the [002] diffraction spot (inset).

taken over 20 tests). Importantly, the yield strength does not appear to correlate with the spread in the initial loading slope. Most likely, the variation in elastic modulus arises due to the combination of three different aspects: i) non-ideal alignment between the nanocrystal and the indenter probe as well as the underlying Si substrate, ii) different motor and thermal drift rates among the tests, and iii) various shape imperfections of the cubes as indicated in the inset in Figure 1c. Aspect (ii) only affects the elastic modulus, while (i) and (iii) can cause changes in the loading slope as well as variations in yield strength through local stress concentrators acting as potential dislocation nucleation sites. However, due to the difficult control of the contact mechanics in nanoscale mechanical testing, a definite reason cannot be given.

Remarkably, the maximum measured axial stress is in excess of 10 GPa, which corresponds to the resolved shear stress of 4.15 GPa assuming a {111} ⟨110⟩ slip system and represents ~37% of the theoretical resolved shear strength (11.2 GPa).[35] Specifically, 10 GPa axial stress along the [001]-axis equates to ca. 57% of the theoretical strength along that direction.[36] To the best of the authors' knowledge, this is the highest experimentally measured strength (G/17) for an $L1_2$ single-crystalline intermetallic. **Table 1** non-exhaustively summarizes the reported Ni_3Al strengths from existing

NANO MICRO small

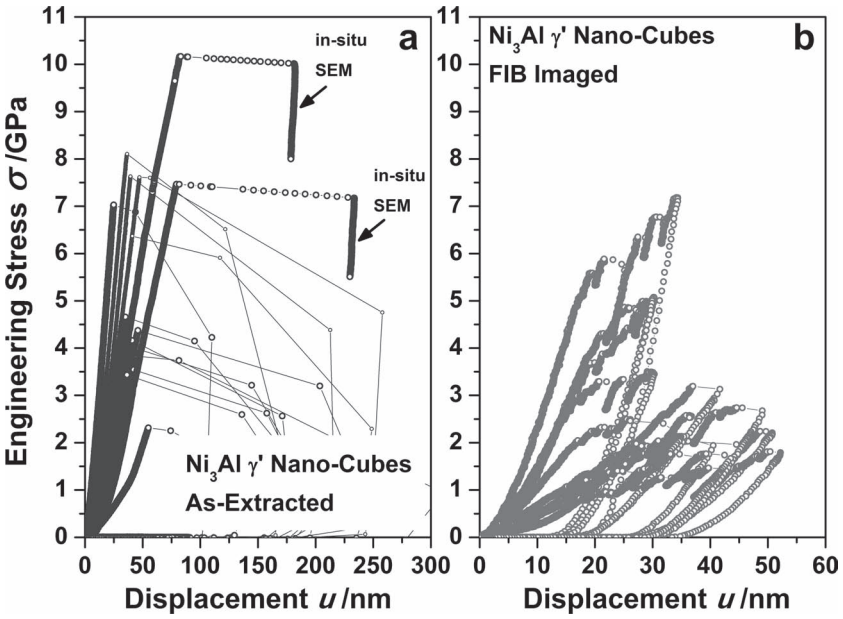

Figure 2. Stress-displacement data for a) as-extracted dislocation-free Ni_3Al crystals, and for b) FIB-imaged crystals. Curves in a) displaying a controlled unload are from in-situ SEM testing.

literature as compared with those for dislocation-free and mobile-dislocation-free fcc, as well as dislocation-free bcc single-crystalline nanostructures.[11,28,37–40]

We also measured the mechanical response of these nanocubes after intentionally exposing them to a single ion rastering scan using 30 keV acceleration voltage, 30 pA current and a magnification of 6000× (~19.5 μm × 21.2 μm scanning area). The stress-displacement data for these samples is shown in Figure 2b, where the *y*-axis scale is identical to the curves plotted in Figure 2a for comparison. It is evident that FIB-exposed samples sustain significantly lower yield stresses, defined as the first resolvable displacement burst longer than ~0.6 nm, with the mean value of 2.23 GPa and a StD of 1.28 GPa over 11 tests. Note that the initial loading slope is scattered similarly to the as-fabricated case. We determine the equivalent ion dose due to FIB exposure to be 0.44 ions nm^{-2}, as calculated by: [equivalent dose = $I \times t_d \times 1/(e \times A_{pixel})$], with I being the current, t_d the dwell time, e the elementary charge, and A_{pixel} the effective area per pixel. It is intriguing that such a small irradiation dose results in a reduction of the average yield strength by ~2.3 GPa, which represents ~50% of the mean. Comparing the strongest specimens from both groups, it becomes apparent that imaging with the ion beam, even at the very low current of 30 pA leads to a reduction in strength by more than 5 GPa. This clearly underlines that the strength of initially dislocation-free fcc nanocrystals is significantly reduced by ion-induced damage, which can take the form of point defects, small dislocation loops and implanted Ga^+-ions, serving as weak dislocation nucleation sites. This finding is consistent with the notion of "upside down" mechanical properties in nanocrystals in the sense that annealing leads to a strength increase while intentional pre-straining (i.e., increased dislocation density) to a weakening.[31] In addition to the large differences in yield strengths, there is also a clear distinction in the flow response between dislocation-free and ion-damaged samples: the typical intermittent stress–strain signature in the latter versus a single catastrophic event leading to failure in the former. These observations are in agreement with those reported for bcc Mo-alloy nanocrystals,[41] and can be rationalized by considering implanted Ga^+-ions and other induced point defects in the sample surface. In fcc metals (pure, ordered and disordered) these surface defects—for example, vacancies—can collapse into prismatic dislocation loops and form dislocation substructures.[42,43] In addition, these irradiation-induced defects may serve as potential sites for dislocation nucleation and multiplication at stresses significantly lower than those required for homogeneous dislocation nucleation, usually on the order of $Gb/2\pi r_c \approx G/10$, with b being the Burgers vector

Table 1. Strength measure for Ni_3Al single crystals and other pristine or mobile-dislocation-free nanocrystals (non-exhaustive). Compressive or tensile strength, σ; resolved shear strength, τ; shear modulus, G.

Material	Crystal Structure	Sample Size	G [GPa]	Largest Measured Stress		Normalized Stress		Ref.
				σ [GPa]	τ [GPa]	σ/G	τ/G	
Ni_3Al[a]	$L1_2$, fcc	Bulk	70.3	0.33	0.15	0.005	0.002	[38]
Ni_3Al[a]	$L1_2$, fcc	2000	70.3	1.17	0.58	0.017	0.008	[37]
Ni_3Al[b]	$L1_2$, fcc	200–600	70.3	3.25	1.32	0.046	0.018	[39]
Ni_3Al	$L1_2$, fcc	200–600	70.3	10.18	4.15	0.145	0.059	this work
Cu[b]	fcc	75–280	30.5	6.19	2.52	0.202	0.083	[11]
Au[c]	fcc	200–1000	40.5	7.60[d]	2.06	0.187	0.051	[40]
Mo[b]	bcc	360–1000	111.5	10.36	4.87	0.093	0.044	[28]

[a]dislocation-containing; [b]pristine, and; [c]mobile-dislocation-free; [d]Note that in this work the stress was estimated from the contact surface of a particle with Winterbottom-like particle shape, thus overestimating the strength somewhat.

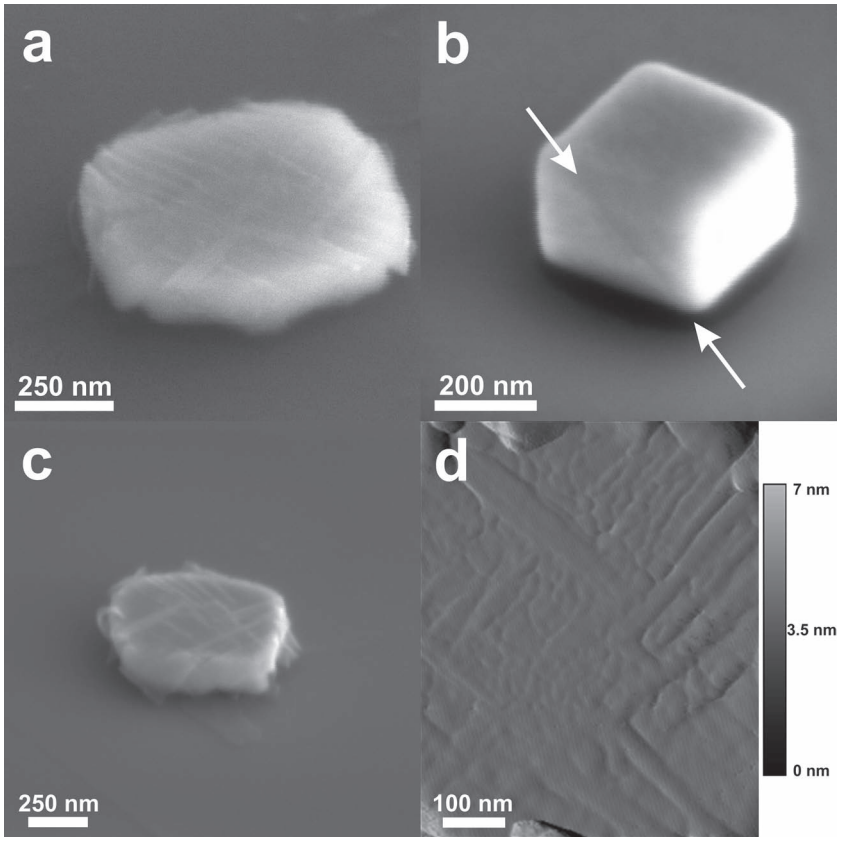

Figure 3. a,c) As-extracted and b) FIB-imaged Ni_3Al nanocrystals after deformation. d) AFM tapping mode image of sample shown in (c). In cases (a,c,d), numerous slip lines and terraces are visible, and the dislocation-free nanocrystals collapse into flats, while FIB-imaged samples display only a few slip lines after deformation and retrain their cubical shape.

and r_c the critical radius for nucleation of a stable dislocation loop.[44] For the Burgers vector of 0.309 nm for Ni_3Al the stress required to expand a typical pre-existing dislocation loop, which we approximate with a circular diameter of 2 nm, is $Gb/(4\pi \times 10^{-9}) \approx 1.7$ GPa, a factor of 4 lower than that required for homogeneous dislocation nucleation. This analysis illustrates that the presence of pre-existing dislocation loops in a crystal, as is the case in FIB-imaged samples, may significantly decrease the observed yield strength. Notably, all of the FIB-imaged nanocubes exhibit a distinctly different signature as compared with the as-extracted ones, implying that here mechanical annealing did not occur, as has been reported in reference [17].

SEM and AFM images in **Figure 3** show sample morphologies after deformation. In conjunction with the instabilities following elastic loading, the as-extracted crystals appear to collapse into flats due to the nano-indenter's inability to maintain the prescribed displacement rate during rapidly occurring post-yield catastrophic failure. A multitude of slip lines can be observed on the surfaces of the dislocation-free samples through SEM images shown in Figure 3a and c, as well as in a tapping-mode AFM image of the same crystal in Figure 3d. The variety of orientations in the slip lines suggests that numerous slip systems were activated, clearly corroborating dislocation mediated plasticity as opposed to brittle fracture observed during tension of Cu nanowhiskers.[11] Interestingly, the clear presence of slip lines here is contrary to earlier work on compression of dislocation-free Mo-alloy bcc nanocrystals,[28] as well as on mobile-dislocation-free yet FIB-less Au fcc microparticles,[40] that do not reveal resolvable slip lines after deformation.

In contrast, the deformed FIB-imaged crystals evidence only a few resolvable slip lines (indicated by the arrows in Figure 3d) and retain their shape integrity. This implies that the underlying dislocation dynamics in the FIB-imaged crystals develop gradually, with dislocations responding to the steadily increasing imposed stress; whereas the as-extracted crystals catastrophically collapse once the applied stress is high enough to nucleate dislocations. Thus, it is reasonable to observe a large distribution of activation stresses in the FIB-imaged crystals due to the induced surface defects.

Figure 4a displays a plot of yield strength as a function of an equivalent length scale for samples with both surface treatments. We define 'size' as the diameter of a circle with an equivalent area and bin nanocubes of similar sizes, resulting in the related measurement uncertainty. By itself, the data obtained in the present study does not cover a large enough size-range to make a conclusive argument on any potential size effect in strength (Figure 4a), yet its apparent but weak slope is in agreement with theoretical predictions for the yield strength of defect free nanosized Ni_3Al pillars.[35] In order to improve our understanding of the possible size-dependence, we combine in Figure 4b literature data for other dislocation-free fcc nanocrystals[11] and mobile-dislocation-free microparticles.[40] Data in this combined plot has been normalized by the material-specific shear moduli and Burgers vectors (0.309 nm/70.3 GPa for Ni_3Al, 0.255 nm/30.5 GPa for Cu, and 0.288/40.5 GPa for Au), an approach utilized in several reviews on this subject.[45,46] In addition, Figure 4b also shows the grey area representing such normalized stresses for defect-containing fcc single crystals taken from the recent review by Greer and de Hosson.[47] Two interesting features become apparent when comparing the combined data of this study with the data obtained in previous studies: 1) the normalized yield stress of dislocation-free crystals is generally higher than that for defect-containing crystals, but more importantly, 2) the data obtained from dislocation-free specimen displays a size-dependence. While it has now been ubiquitously demonstrated that the power-law exponent n of $\tau \propto (d/b)^{-n}$, with d being the sample dimensions, describing the size-dependence of dislocation-containing crystals, is on the order of –0.6, we choose not to fit the data for our dislocation-free crystals

NANO MICRO small

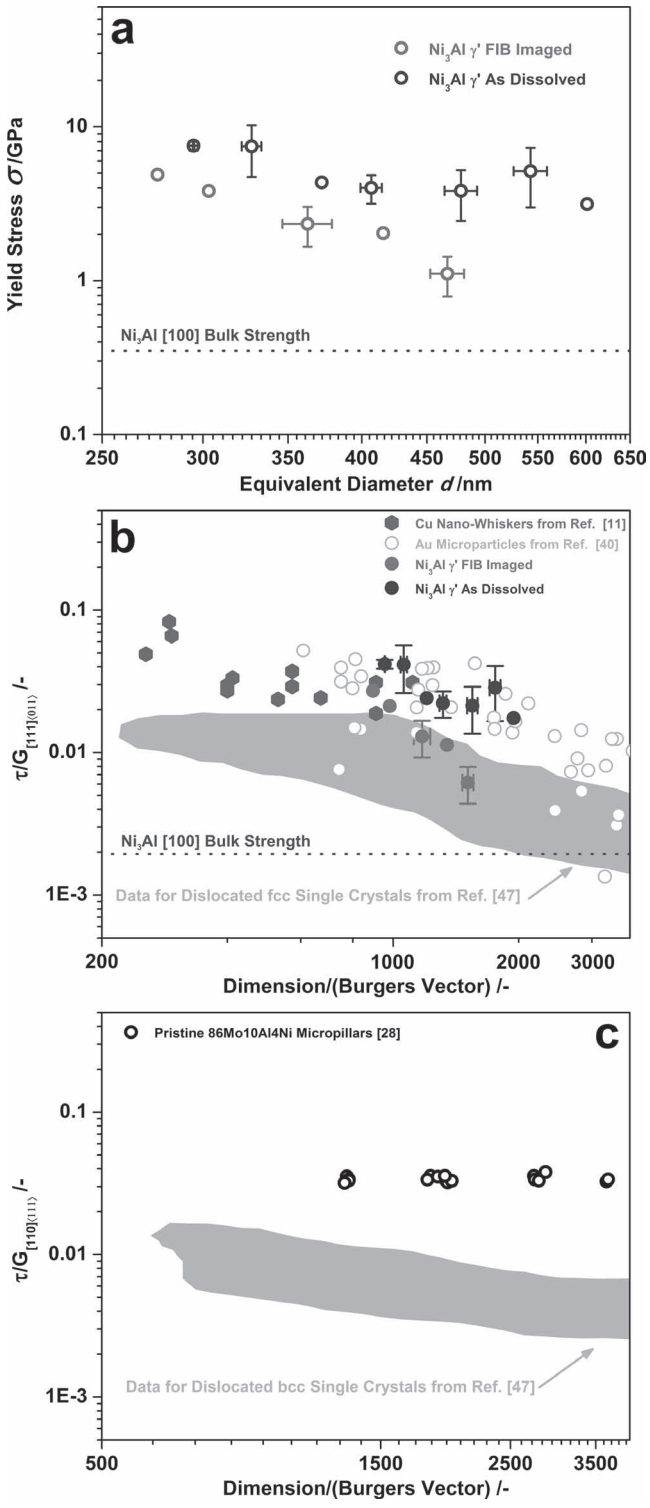

Figure 4. a) Yield-stress as a function of equivalent diameter clearly revealing a size effect for FIB imaged Ni_3Al nanocubes, whereas the data of the as-extracted Ni_3Al nanocubes has, if at all, a weak size-dependence. b) Combined plot of literature data on other fcc nanocrystals (grey area corresponds to those reported for defect-containing nanocrystals). The bulk strength for a [001]-oriented Ni_3Al crystal is also provided for comparison.[38] c) Displays the same type of plot as in (b) but for bcc nanocrystals. Both (b) and (c) have the same *y*-axis scaling and the same *x*-range in order to facilitate comparison.

as the scatter and the limited size-range may be misleading in precise determination of the slope. Although the combined data of dislocation-free Cu whiskers[11] and our dislocation-free Ni_3Al nanocubes cover a size-range of one magnitude, a range generally suitable for size dependence evaluation, we exercise caution in observing that upon removal of, for instance, the three smallest-diameter data points for Cu, the slope is dramatically reduced, if present at all. Additional data is necessary to explore the intriguing trend depicted in Figure 4b, which clearly appears to be less definite in comparison to the same type of plot but for bcc nanocrystals depicted in Figure 4c.

Exploring the origins of the implied size-dependence of the dislocation-free fcc nanocrystals captured in Figure 4b, in combination with their attainment of close-to-theoretical yield stresses, and the presence of nontrivial scatter in the strength data, naturally evokes the picture of surface dislocation nucleation as the likely governing plasticity mechanism. The sources of scatter include sample geometry imperfections, generating local stress concentrators, which subsequently lead to surface dislocation nucleation. This notion also provides the basis for the weakest-link model (Weibull statistics) proposed by Kraft et al.,[48] whereby the strength scales with volume and/or surface area considering a statistical distribution of surface defects.[48,49] As gleaned from molecular dynamics simulations, nanometer-sized Ni_3Al and Au crystals have the propensity for nucleating Shockley partials at a strain, where the local atomic thermal vibrations exceed some critical threshold.[35,50] Additional evidence for surface controlled dislocation nucleation mechanisms arising at this size-scale has recently been proposed based on experimental data in conjunction with simulations obtained from mobile-dislocation-free Au microparticles.[40]

In the context of the current understanding of nanoscale fcc plasticity, our findings clearly support the emerging presupposition that size-dependent scaling of nanoscopic fcc crystals is not universal with respect to the underlying governing dislocation mechanisms, but rather depends on the initial defect structure. This, in combination with the continued search for fundamental physical origins of size-dependent strengths in nanocrystals, forms the basis for future experimental challenges of plasticity at the nanoscale.

Experimental Section

Sample Preparation: Discs with 2 mm thickness and 5 mm diameter were cut from a commercial standard heat treated CMSX-4 Ni-based bulk superalloy; more details are in the literature.[51] Its microstructure consists of a uni-modal distribution of cuboidal $Ni_3(Al,X)$ γ' precipitates ($L1_2$, cP4 structure with cubic symmetry) with coherent interfaces and edge lengths measuring between 200 and 500 nm, where X may be any other of bulk alloy's elements. For simplicity, we refer to the material as Ni_3Al hereafter. We note that this γ' phase possesses an ordered fcc arrangement and deforms on the {111} ⟨110⟩ slip system at ambient temperatures.[52] The discs were electrochemically etched in an aqueous electrolyte (H_3PO_4:methanol = 1:2) with a voltage of 6 V, so that the matrix

phase (γ) was selectively etched away. After partially etching away the matrix, the discs were soaked in an ultrasonic methanol bath and the extracted γ' nanocubes were collected from the solution by centrifugal force and then soaked in an ethanol solution again. The obtained suspension of Ni_3Al γ' nanocubes was subsequently applied as droplets onto a single-crystalline silicon wafer, resulting in free standing nanocubes.

Sample Characterization: TEM (Tecnai TF20, double tilt holder, 200 kV) was used to investigate the initial microstructure of both Ni_3Al nanocubes and the bulk crystal from which they were extracted. The TEM foils were prepared by either low-energy FIB milling (FEI Nova 200, 10 keV and 3 pA) or by conventional electropolishing.

Nanomechanical Testing: Mechanical testing was conducted in the Hysitron Triboscope nano-indenter equipped with a 8-μm-diameter flat-punch probe serving as compression anvil, as well as in SEMentor, a custom-made in-situ nanomechanical instrument comprised of the dynamic contact module (DCM) similar to a nano-indenter (Agilent Corp.) but inside of a field-emission SEM (FEI Quanta 200).[53] Both devices operated in closed loop displacement controlled conditions. In-situ testing was conducted in order to have a better control of the contact between the tip and the specimen, as well as to observe the structural collapse of the nanocubes. All nanocubes were compressed at a constant displacement rate of 2 nm s^{-1} in the Hysitron indenter and at the strain rate of 10^{-3} s^{-1} during in-situ SEM testing. Engineering stresses were calculated by using the nanocubes top area as sample cross-section. Note that we only rely on stress data acquired prior to the catastrophic event displayed in Figure 2a because the catastrophic collapse of the structures lead to uncontrollable conditions for the feedback control of both devices used.

Acknowledgements

R.M. gratefully acknowledges the financial support of the Alexander von Humboldt foundation, as well as his host G.M. Pharr for fruitful discussions. The authors thank D. Jang for experimental TEM support. J.R.G. is thankful for the financial support of the Office of Naval Research (ONR Grant N000140910883).

[1] M. D. Uchic, D. M. Dimiduk, J. N. Florando, W. D. Nix, *Science* **2004**, *305*, 986–989.
[2] J. R. Greer, W. C. Oliver, W. D. Nix, *Acta Mater.* **2005**, *53*, 1821–1830.
[3] A. S. Schneider, D. Kaufmann, B. G. Clark, C. P. Frick, P. A. Gruber, R. Monig, O. Kraft, E. Arzt, *Phys. Rev. Lett.* **2009**, *103*, 105501.
[4] S. Brinckmann, J. Y. Kim, J. R. Greer, *Phys. Rev. Lett.* **2008**, *100*, 155502.
[5] J. R. Greer, C. R. Weinberger, W. Cai, *Mater. Sci. Eng. A* **2008**, *493*, 21–25.
[6] C. R. Weinberger, W. Cai, *Proc. Natl. Acad. Sci. USA* **2008**, *105*, 14304–14307.
[7] R. Maass, S. Van Petegem, D. Ma, J. Zimmermann, D. Grolimund, F. Roters, H. Van Swygenhoven, D. Raabe, *Acta Mater.* **2009**, *57*, 5996–6005.
[8] D. Kiener, P. J. Guruprasad, S. M. Keralavarma, G. Dehm, A. A. Benzerga, *Acta Mater.* **2011**, *59*, 3825–3840.
[9] C. A. Volkert, E. T. Lilleodden, *Phil. Mag.* **2006**, *86*, 5567–5579.
[10] C. A. Volkert, E. T. Lilleodden, D. Kramer, J. Weissmueller, *Appl. Phys. Lett.* **2006**, *89*, 061920.
[11] G. Richter, K. Hillerich, D. S. Gianola, R. Monig, O. Kraft, C. A. Volkert, *Nano Lett.* **2009**, *9*, 3048–3052.
[12] C. P. Frick, B. G. Clark, S. Orso, A. S. Schneider, E. Arzt, *Mater. Sci. Eng. A* **2008**, *489*, 319–329.
[13] A. S. Schneider, C. P. Frick, B. G. Clark, P. A. Gruber, E. Arzt, *Mater. Sci. Eng. A* **2011**, *528*, 1540–1547.
[14] J.-Y. Kim, J. R. Greer, *Acta Mater.* **2009**, *57*, 5245–5253.
[15] S. H. Oh, M. Legros, D. Kiener, G. Dehm, *Nat. Mater.* **2009**, *8*, 95–100.
[16] A. M. Minor, S. A. S. Asif, Z. W. Shan, E. A. Stach, E. Cyrankowski, T. J. Wyrobek, O. L. Warren, *Nat. Mater.* **2006**, *5*, 697–702.
[17] Z. W. Shan, R. K. Mishra, S. A. S. Asif, O. L. Warren, A. M. Minor, *Nat. Mater.* **2008**, *7*, 115–119.
[18] R. Maass, S. Van Petegem, C. N. Borca, H. Van Swygenhoven, *Mater. Sci. Eng. A* **2009**, *524*, 40–45.
[19] R. Maass, S. Van Petegem, D. Grolimund, H. Van Swygenhoven, M. D. Uchic, *Appl. Phys. Lett.* **2007**, *91*, 131909.
[20] R. Maass, S. Van Petegem, D. Grolimund, H. Van Swygenhoven, D. Kiener, G. Dehm, *Appl. Phys. Lett.* **2008**, *92*, 071905.
[21] R. Maass, M. D. Uchic, *Acta Mater.* **2012**, *60*, 1027–1037.
[22] D. Kiener, C. Motz, M. Rester, M. Jenko, G. Dehm, *Mater. Sci. Eng. A* **2007**, *459*, 262–272.
[23] J. R. Greer, W. D. Nix, *Phys. Rev. B* **2006**, *73*, 245410.
[24] H. Bei, S. Shim, *Appl. Phys. Lett.* **2007**, *91*, 111915.
[25] R. Maass, D. Grolimund, S. Van Petegem, M. Willimann, M. Jensen, H. Van Swygenhoven, T. Lehnert, M. A. M. Gijs, C. A. Volkert, E. T. Lilleodden, R. Schwaiger, *Appl. Phys. Lett.* **2006**, *89*, 151905.
[26] A. T. Jennings, M. J. Burek, J. R. Greer, *Phys. Rev. Lett.* **2010**, *104*, 135503.
[27] M. Dietiker, S. Buzzi, G. Pigozzi, J. F. Loffler, R. Spolenak, *Acta Mater.* **2011**, *59*, 2180–2192.
[28] H. Bei, S. Shim, E. P. George, M. K. Miller, E. G. Herbert, G. M. Pharr, *Scr. Mater.* **2007**, *57*, 397–400.
[29] H. Bei, S. Shim, G. M. Pharr, E. P. George, *Acta Mater.* **2008**, *56*, 4762–4770.
[30] P. S. Phani, K. E. Johanns, G. Duscher, A. Gali, E. P. George, G. M. Pharr, *Acta Mater.* **2011**, *59*, 2172–2179.
[31] S. W. Lee, S. M. Han, W. D. Nix, *Acta Mater.* **2009**, *57*, 4404–4415.
[32] R. C. Reed, *The Superalloys: Fundamentals and Applications*, Cambridge University Press, Cambridge, UK **2006**.
[33] T. M. Pollock, A. S. Argon, *Acta Metall. et Mater.* **1992**, *40*, 1–30.
[34] T. Link, A. Epishin, U. Bruckner, P. Portella, *Acta Mater* **2000**, *48*, 1981–1994.
[35] L. Zuo, A. H. W. Ngan, *Phil. Mag. Lett.* **2006**, *86*, 355–365.
[36] M. Sob, M. Friak, D. Legut, J. Fiala, V. Vitek, *Mater. Sci. Eng. A* **2004**, *387*, 148–157.
[37] M. D. Uchic, M. A. Groeber, D. M. Dimiduk, J. P. Simmons, *Scr. Mater.* **2006**, *55*, 23–28.
[38] F. E. Heredia, D. P. Pope, *Acta Metall. et Mater.* **1991**, *39*, 2017–2026.
[39] J. Schloesser, J. Rösler, D. Mukherji, *Int. J. Mater. Res.* **2011**, *102*, 532.
[40] D. Mordehai, S.-W. Lee, B. Backes, D. J. Srolovitz, W. D. Nix, E. Rabkin, *Acta Mater.* **2011**, *59*, 5202–5215.
[41] S. Shim, H. Bei, M. K. Miller, G. M. Pharr, E. P. George, *Acta Mater.* **2009**, *57*, 503–510.
[42] J. P. McCaffrey, M. W. Phaneuf, L. D. Madsen, *Ultramicroscopy* **2001**, *87*, 97–104.
[43] D. J. Barber, *Ultramicroscopy* **1993**, *52*, 101–125.
[44] D. Hull, D. J. Bacon, *Introduction to Dislocations*, 4th ed., Butterworth Heinemann, Oxford **2001**.
[45] R. Dou, B. Derby, *Scripta Mater.* **2009**, *61*, 524–527.
[46] M. D. Uchic, P. A. Shade, D. M. Dimiduk, *Ann. Rev. Mater. Sci.* **2009**, *39*, 361–386.

[47] J. R. Greer, J. T. M. De Hosson, *Prog. Mater. Sci.* **2011**, *56*, 654–724.
[48] O. Kraft, P. A. Gruber, R. Moenig, D. Weygand, *Ann. Rev. Mater. Res.* **2010**, *40*, 293–317.
[49] A. H. W. Ngan, L. Zuo, P. C. Wo, *Proc. R. Soc. A - Math. Phys. Eng. Sci.* **2006**, *462*, 1661–1681.
[50] E. Rabkin, D. J. Srolovitz, *Nano Lett.* **2007**, *7*, 101–107.
[51] K. Harris, *Superalloys*, Warrendale, PA, **1992**.
[52] J. H. Westbrook, in *Dislocations in Solids;* Vol. *10* (Eds: F. R. N. Nabarro, M. S. Duesbery), Elsevier, **1996**, p. 1–26.
[53] J.-Y. Kim, D. Jang, J. R. Greer, *Scr. Mater.* **2009**, *61*, 300–303.

Received: December 12, 2011
Published online: March 27, 2012

